THE JOURNAL OF BIOLOGICAL CHEMISTRY Vol. 279, No. 35, Issue of August 27, pp. 37175–37184, 2004
Printed in U.S.A.

Human DNA Methyltransferase 1 Is Required for Maintenance of the Histone H3 Modification Pattern*

Received for publication, April 30, 2004, and in revised form, June 23, 2004
Published, JBC Papers in Press, June 25, 2004, DOI 10.1074/jbc.M404842200

Jesus Espada‡§, Esteban Ballestar‡, Mario F. Fraga‡, Ana Villar-Garea‡, Angeles Juarranz¶, Juan C. Stockert¶, Keith D. Robertson‖, François Fuks, and Manel Esteller‡ ‡‡**

*From the ‡Epigenetics Laboratory, Spanish National Cancer Centre (CNIO), Melchor Fernandez Almagro 3, 28029 Madrid, Spain, the ¶Department of Biology, Faculty of Sciences, Autonomous University of Madrid, Cantoblanco, 28049 Madrid, Spain, ‖Epigenetic Gene Regulation and Cancer Section, NCI, National Institutes of Health, Bethesda, Maryland 20892, and **Free University of Brussels, Laboratory of Molecular Virology, Faculty of Medicine, 808 Route de Lennik, 1070 Brussels, Belgium*

DNA methyltransferase 1 (DNMT1) plays an essential role in murine development and is thought to be the enzyme primarily responsible for maintenance of the global methylation status of genomic DNA. However, loss of DNMT1 in human cancer cells affects only the methylation status of a limited number of pericentromeric sequences. Here we show that human cancer cells lacking DNMT1 display at least two important differences with respect to wild type cells: a profound disorganization of nuclear architecture, and an altered pattern of histone H3 modification that results in an increase in the acetylation and a decrease in the dimethylation and trimethylation of lysine 9. Additionally, this phenotype is associated with a loss of interaction of histone deacetylases (HDACs) and HP1 (heterochromatin protein 1) with histone H3 and pericentromeric repetitive sequences (satellite 2). Our data indicate that DNMT1 activity, via maintenance of the appropriate histone H3 modifications, contributes to the preservation of the correct organization of large heterochromatic regions.

Methylation of CpG dinucleotides is an epigenetic phenomenon involved in regulating important intranuclear events, such as the organization of chromatin structure, transcriptional control, and replication timing (1). The process is characterized by the transfer of methyl groups to the C-5 position of cytosine and is catalyzed by members of the DNA methyltransferase (DNMT)[1] protein family. To date, five mammalian DNMTs have been identified as follows: DNMT1, DNMT3a, DNMT3b, DNMT2, and DNMT3L (1). Of these five, DNMT1, DNMT3a, and DNMT3b are known to be essential for proper development in murine knockout models (1–3). DNMT1, the most abundant DNA methyltransferase in somatic cells, has a strong preference for hemimethylated DNA and is therefore believed to be the enzyme primarily responsible for copying and maintaining methylation patterns from the parental to the daughter strand following DNA replication (1). Strikingly, significant genomic hypomethylation was only found at pericentromeric satellite 2 and 3 sequences in human cancer cells lacking DNMT1 (KO1 cells) (4). This suggests the possibility of regional specificity on the part of DNMT1 and, furthermore, that DNMT1 loss might be partially compensated by other DNMTs (4).

Accumulated evidence suggests that DNA methylation status and changes in the biochemical modification of histone tails, the "histone code," can regulate the higher order organization and function of large intranuclear regions, implicating these modifications in chromosome positioning and the maintenance of specific chromatin domains within the nucleus in a wide variety of organisms (5–10). Recent data from plant cells indicate that loss of methylated CpG dinucleotides alters the methylation pattern of histone H3 (11), suggesting that DNA methylation may also function as a central signal for the regulation of chromatin structure. A reciprocal dependence may exist, because mouse embryonic stem cells lacking Suv39h histone methyltransferases display an altered DNA methylation profile at pericentric satellite repeats (12). In order to determine the significance of DNA methylation with regard to chromatin and nuclear organization in humans, we used KO1 cells to investigate the consequences of a loss of methylation in a large but well defined intranuclear region, pericentromeric repeats.

EXPERIMENTAL PROCEDURES

Cell Culture, Cell Cycle Analysis, and Cell Transfections—Human HCT-116 colon cancer cells (WT cells) and HCT116 knockout cells lacking DNMT1 (KO1) (4) were grown in McCoy's 5A culture medium supplemented with 10% fetal bovine serum (Invitrogen). KO1 cells were also supplemented with 0.1 mg/ml hygromycin B (Sigma). All analyses were carried out before passage 22. For cell cycle analysis, cells were trypsinized, slowly resuspended in 70% ethanol in PBS at 4 °C for 5 min, washed in PBS, and incubated for 30 min in PBS containing 0.05 mg/ml propidium iodide (Sigma) and 1 mg/ml RNase I (Sigma). The cell suspension was then analyzed by FACSCalibur (BD Biosciences). TUNEL assays (Roche Applied Science) were performed in early subconfluent cells following the instructions of the manufacturer.

For re-expression of DNMT1, KO1 cells were cotransfected with a pcDNA3.1/B plasmid (Invitrogen) containing the murine DNMT1 cDNA (13). Transfections were performed with LipofectAMINE PLUS reagent (Invitrogen) following the manufacturer's instructions. Twenty four hours after transfection, cells were treated with 1.6 μg/ml puromycin (Sigma) for at least 1 week. Stocks of resistant cells expressing the murine DNMT1 were selected for further studies.

* This work was supported by the Departments of Science and Health of the Spanish Government and Grant CAM08.1/0010.1/2001. The costs of publication of this article were defrayed in part by the payment of page charges. This article must therefore be hereby marked "*advertisement*" in accordance with 18 U.S.C. Section 1734 solely to indicate this fact.

§ Postdoctoral Fellow of the Ayuntamiento de Madrid.

‡‡ To whom correspondence should be addressed: Epigenetics Laboratory, Spanish National Cancer Centre (CNIO), Melchor Fernandez Almagro 3, 28029 Madrid, Spain. Tel.: 34-91-2246940; Fax: 34-91-2246923; E-mail: mesteller@cnio.es.

[1] The abbreviations used are: DNMT, DNA methyltransferase; 5mC, 5-methylcytosine; HDAC, histone deacetylase; ChIP, chromatin immunoprecipitation; PBS, phosphate-buffered saline; DAPI, 4,6-diamidino-2-phenylindole; WT, wild type; HPLC, high performance liquid chromatography; TUNEL, terminal dUTP nick-end labeling; HPCE, high performance capillary electrophoresis; MNase, micrococcal nuclease; HMTase, histone methyltransferase; MEFs, mouse embryo fibroblasts; Sat2, satellite 2.

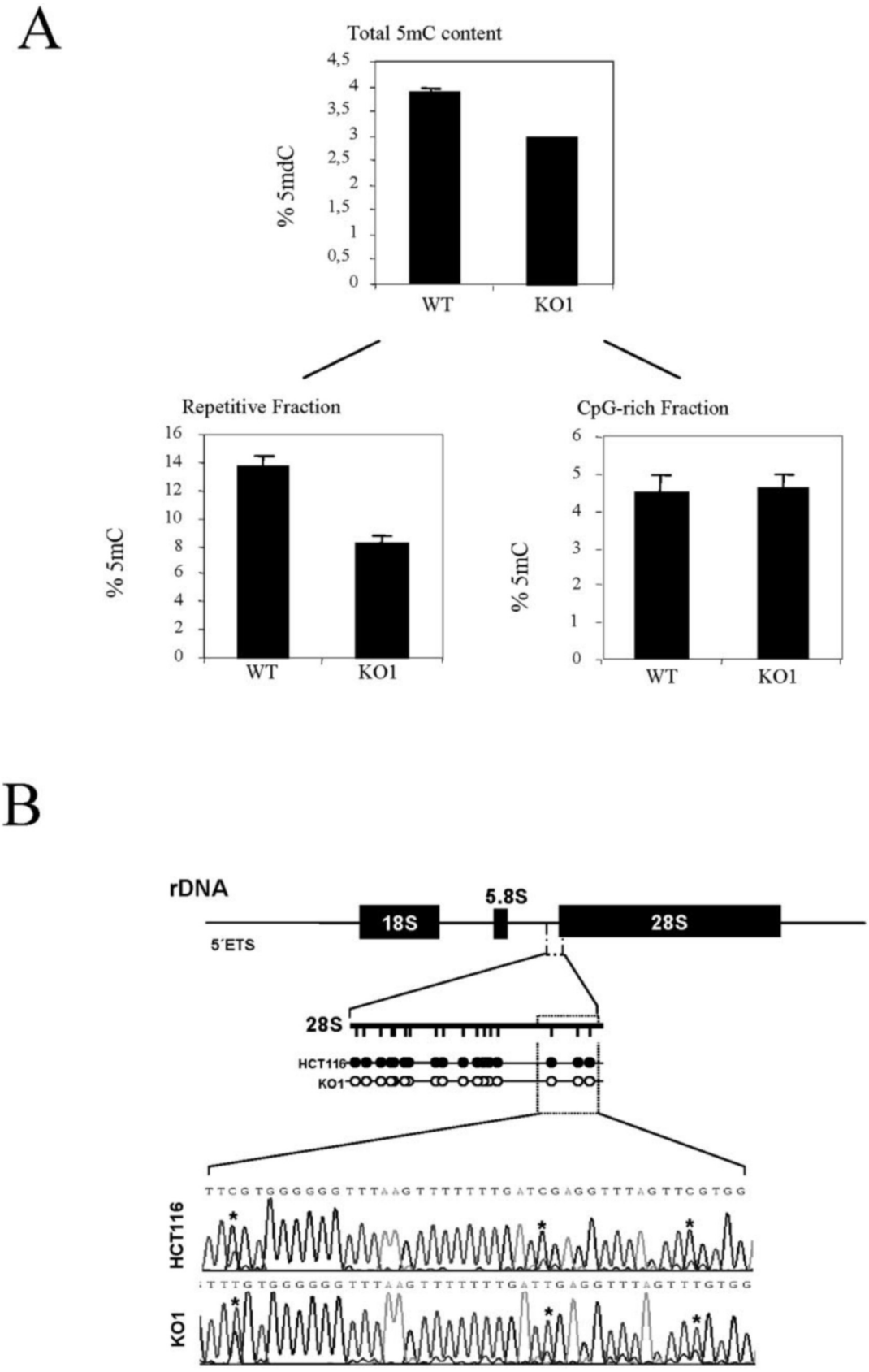

FIG. 1. **Specific loss of 5mC in repetitive genomic sequences in human cells lacking DNMT1.** *A*, quantitative analysis of total 5mC content in wild type (*WT*) and DNMT1 knockout (*KO1*) cells and the distribution of the 5mC content in repetitive and CpG-rich genomic fractions, as described under "Experimental Procedures." *B*, bisulfite genomic sequencing of the 5′-end of the 28 S component of ribosomal DNA. Schematic representation of the CpG sites included the PCR fragment, demonstrating methylation in the HCT-116 wild type cell line (retention of cytosine,"Cs") and demethylation in the KO1 cells (transformation to thymines, "Ts"). *Black circles* indicate methylated CpGs; *white circles* indicate unmethylated CpGs.

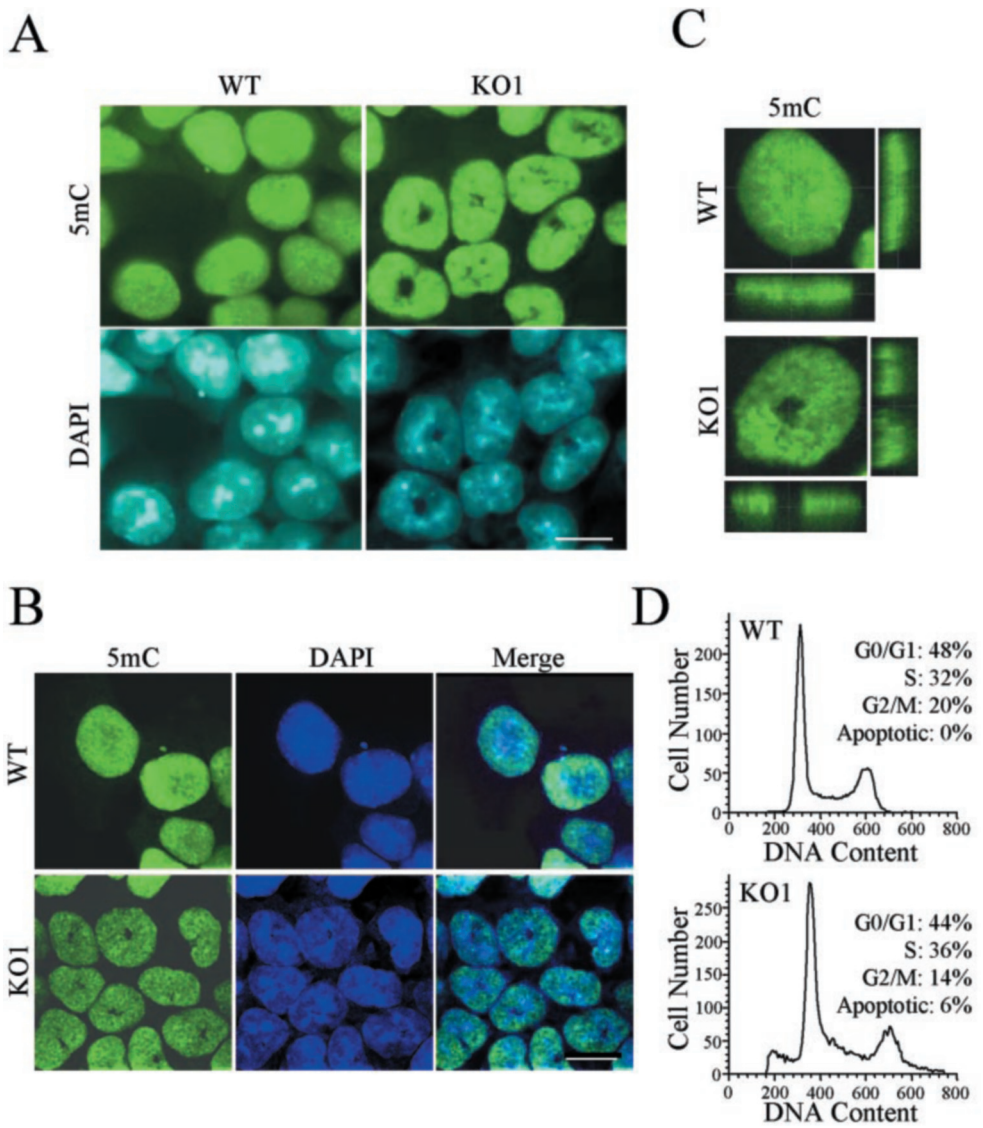

FIG. 2. **Alterations of the nuclear morphology without changes in the cell cycle in human cells lacking DNMT1.** *A*, immunofluorescence analysis of the distribution of 5mC (*top panel*) and DAPI-stained DNA (*bottom panel*) shows altered heterochromatin distribution and the appearance of nuclear morphologic alterations in KO1 cells compared with WT cells. *B*, colocalization analysis in 0.2-μm thick confocal sections of 5mC (*left panel*) and DAPI-stained DNA (*middle panel*) in WT and KO1 cells. *Bars*, 10 μm. *C*, orthogonal reconstruction of 5mC distribution in single WT and KO1 nuclei on the horizontal plane. *D*, cell cycle analysis of WT and KO1 cells. Propidium iodide-stained DNA contents in fixed cells were analyzed by flow cytometry. The percentages of cells in various cell cycle phases are indicated.

Nuclear Extracts—Trypsinized cells were washed in PBS, resuspended in 10 volumes of cell lysis buffer (0.65 M sucrose, 20 mM Tris, pH 8, 10 mM $MgCl_2$, 2% Triton X-100), and incubated on ice for 15 min. Cells were then centrifuged at 1500 rpm for 5 min, and the nuclear pellet was resuspended in 1 ml of NT buffer (50 mM Tris, pH 7.4, 100 mM NaCl, 5 mM $MgCl_2$, 5 mM $CaCl_2$, 1% Nonidet P-40, 1% Triton X-100) containing 10 units of DNase I (TURBO DNase, Ambion), plus protease and phosphatase inhibitors (2 mM phenylmethylsulfonyl fluoride, 20 μg/ml aprotinin, 1 mM sodium orthovanadate). Samples were incubated on ice for 20 min and then centrifuged at 13,000 rpm at 4 °C for 15 min.

Antibodies and Immunological Methods—The following antibodies were used: rabbit polyclonal antibodies raised against acetyl-Lys-9 histone H3 (Upstate Biotechnologies, Inc.); trimethyl-Lys-9 histone H3 (generously provided by Dr. Thomas Jenuwein) (14); dimethyl-Lys-9 histone H3, HDAC-1, and HDAC-2 (Abcam); HP1α (Euromedex); mouse monoclonal antibodies against histone H3 (Upstate Biotechnologies, Inc.); and 5-methylcytosine (5mC) (a generous gift from Dr. A. Niveleau). Secondary antibodies used included anti-mouse and anti-rabbit IgG horseradish peroxidase conjugates (Amersham Biosciences), anti-mouse IgG Cy3-conjugate, and anti-rabbit IgG Cy2 conjugate (Jackson ImmunoResearch). Immunoprecipitation and immunoblotting of nuclear protein extracts were performed as described (15).

Standard chromatin immunoprecipitation (ChIP) assays were performed as described previously (16, 17). When investigating HDAC association, prior to formaldehyde cross-linking, cells were also treated with the protein-protein cross-linking agent dimethyl adipimidate (10 mM in PBS containing 0.25% Me_2SO) for 45 min (18). Chromatin was sheared by sonication with a Branson Sonifier 250 to an average length of 0.25–1.0 kb. PCR amplification was performed in 25-μl volumes with primers specific for each promoter analyzed. For each of these, the linear range of PCR amplification was evaluated empirically by serial dilution of total DNA collected after sonication (input fraction). This previous titration step yields semiquantitative PCR data (with an approximate error of 10–20%), which is generally sensitive enough to allow changes in histone modifications and association of nuclear factors to be monitored. Primers used are as follows: 5′-TCG CAT AGA ATC GAA TGG AA-3′ (sense) and 5′-GCA TTC GAG TCC GTG GA-3′ (antisense) for satellite 2; and 5′-CTC AGC GAG GAA GAA TAC CG-3′ (sense) and 5′-ACC GGG CCT AGA CCT AGA AG-3′ (antisense) for D4Z4.

Immunofluorescence—Cells were grown on coverslips in P60 dishes, fixed in 4% formaldehyde, and stained as described previously (15). Cells to be analyzed for 5mC were postfixed in cold methanol, treated with 1 M HCl at 37 °C for 30 min, and stained as described by Habib *et al.* (19). Confocal optical sections were obtained using a Leica TCS SP microscope (Leica Microsystems) equipped with krypton and argon lasers. Images were acquired with Leica LCS Lite software and processed with Adobe Photoshop 5.0 (Adobe Systems Inc.) and publicly

available NIH image software. The values obtained correspond to the integrated density of the total fluorescent emission per nuclear area of the signals in 50 nuclei from each experiment. Values, in arbitrary units, are shown as averages (± S.D.).

Electron Microscopy—Cells were grown to subconfluence in F-25 flasks, washed in 0.1 M sodium cacodylate, and fixed in a solution of 2% glutaraldehyde and 4% paraformaldehyde in 0.1 M sodium cacodylate for 1 h at 4 °C. Samples were treated postfixation with 1% OsO_4 and 1% $K_3Fe(CN)_6$. After three washes with sodium cacodylate, samples were dehydrated with ethanol, treated with propylene oxide, and embedded in Epon (Resolution Performance Products). Ultrathin sections were prepared, contrasted with uranyl acetate and lead citrate, and examined at 80 kV under a JEOL 1010 electron microscope.

Quantification of Whole Histone Acetylation by High Performance Capillary Electrophoresis (HPCE)—The degree of histone H3 acetylation was measured by a modification of methods described previously (20). Briefly, cell nuclei were obtained as described (21), and histones were extracted by acid extraction with the addition of 0.25 M HCl followed by acetone precipitation. Histones were fractionated by reverse-phase high performance liquid chromatography (HPLC) (Beckman-Coulter) on a Delta-Pak C18 column (Waters) and eluted with an acetonitrile gradient (20–60%) in 0.3% trifluoroacetic acid using an HPLC gradient system. Histone purity was tested by SDS-PAGE. The non-, mono-, di-, tri-, and tetra-acetylated derivatives of the H3 fraction were resolved by HPCE.

Quantification of Genomic 5mC Content by HPCE—The degree of methylation was determined essentially as described by Fraga *et al.* (22) with minor modifications. Genomic DNA (150 μg) was first treated with the 4-base frequent cutter MseI. This endonuclease digests genomic DNA into 100–200-bp fragments. Its recognition sequence, TTAA, rarely occurs within GC-rich regions, leaving most CpG islands (700–1200 bp on average) intact (23, 24). MseI-digested DNA was fractionated by using 2% agarose gel electrophoresis, and DNA fragments of ~200–400, 700–1200, and 1800–2100 bp were purified from the gels. As demonstrated by PCR, the 200–400- and 1800–2100-bp fractions were enriched in different genomic repeats, like the Alu8 and Alu4 family of retrotransposon-derived repeats, the satellite 2 tandem repeat, the minisatellite single-sequence repeat, and the ribosomal DNA gene tandem repeat. None of these sequences was present in the 700–1200-bp fraction, and the 200–400- and 1800–2100-bp fractions were defined as the repetitive fraction. On the other hand, it was established by PCR that the 700–1200-bp fraction mainly contained CpG islands such as the promoter region of the androgen receptor, RAS association domain family 1A (RASSF1A), and the E-cadherin (*CDH1*) genes. Primer sequences and PCR conditions are available upon request. These sequences were not present in the repetitive fraction, and the 700–1200-bp fraction was defined as the CpG fraction. Most interestingly, the D4Z4 repeat was mainly contained in the CpG fraction. Each DNA fraction was purified using the QIAquick gel extraction kit (Qiagen), and then DNA was enzymatically hydrolyzed with nuclease P1 and alkaline phosphatase (Sigma) and directly injected in a CE system (P/ACE™ MDQ, Beckman-Coulter) connected to a data processing station (32 Karat™ software) equipped with an uncoated fused silica capillary (BD Biosciences) (60.2 cm × 75 μm, effective length, 50 cm). The running buffer was 14 mM $NaHCO_3$, pH 9.6, containing 20 mM SDS. Running conditions were 25 °C and an operating voltage of 17 kV. On-column absorbance was monitored at 254 nm. All samples were analyzed in duplicate, and three analytical measurements were made per replicate. Quantification of the relative methylation of each DNA sample was determined as the percentage of mC of total cytosines: mC peak area × 100/(C peak area + mC peak area).

Bisulfite Genomic Sequencing—We carried out bisulfite modification of genomic DNA as described previously (25). The DNA methylation status at the 5′-end of the 28 S component of ribosomal DNA was analyzed by bisulfite genomic sequencing of their corresponding CpG islands, as described by Paz *et al.* (25). Both strands were sequenced. The primer sequences used are as follows: 5′-GAG TGA ATA GGG AAG AGT TTA G-3′ (sense) and 5′-AAA ATT CTT TTC AAC TTT CCC TTA C-3′ (antisense). PCR conditions for the methylation analysis are available upon request.

Micrococcal Nuclease Analysis—Accessibility to micrococcal nuclease in wild type and KO1 HCT116 cells was investigated. Cells were lysed by incubation with cold RSB buffer (10 mM Tris, pH 7.5, 10 mM NaCl, 3 mM $MgCl_2$) in the presence of protease inhibitors for 10 min. Once the nuclei had been isolated, the nuclear pellet was resuspended with wash buffer of 15 mM HEPES, pH 7.4, 15 mM NaCl, 60 mM KCl, 2 mM $MgCl_2$, preincubated at 37 °C, and digested with micrococcal nuclease (MNase) (20 units/ml) after addition of 0.2 mM $CaCl_2$. Two chromatin fractions were analyzed as follows: whole genomic DNA, obtained when directly extracting DNA from each sample, and soluble chromatin, containing mainly mononucleosomes, when centrifuging the cells after digestion and isolating the DNA from the supernatant.

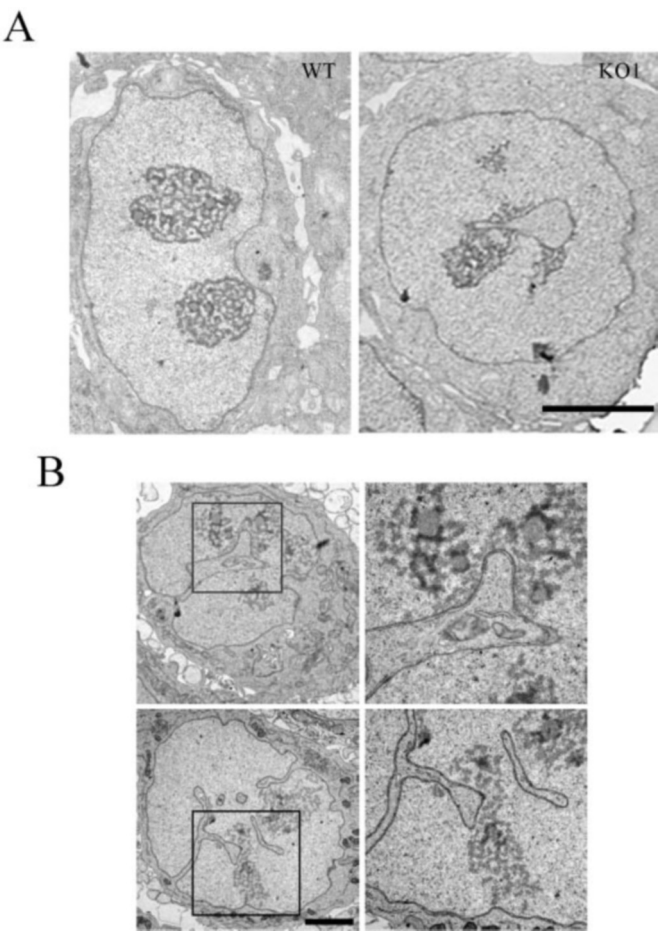

FIG. 3. **Electron microscopy analysis of human cells lacking DNMT1.** *A*, general morphology of WT and KO1 cells at the electron microscopic level showing the aberrant nuclear morphology associated with the loss of DNMT1. Note that the nucleolar substructure is similar in both cell types. However, WT cells contain spherically shaped nucleoli, whereas KO1 cells show deformed nucleolar masses frequently attached to a deep invagination of the nuclear envelope. *Bar*, 5 μm. *B*, electron micrographs of KO1 cells showing numerous deformations and folds of the nuclear envelope to which distorted nucleoli are attached. Images in *right panels* correspond to the *highlighted squares* in *left panels. Bar*, 2.5 μm.

RESULTS

Specific Loss of Cytosine Methylation in Repetitive Genomic Sequences in Human Cells Lacking DNMT1—We initially analyzed the total content and the biochemical distribution of 5mC in distinct genomic fractions in both wild type (WT) HCT-116 and KO1 cells. In accordance with data reported previously, we confirmed a reduction of only 20% in the total 5mC content in KO1 cells compared with WT cells (4) (Fig. 1). However, when genomic DNA was separated into two major fractions, consisting of repetitive sequences (repetitive fraction) and CpG islands (CpG-rich fraction; see "Experimental Procedures") before the analysis of the 5mC content, we observed that the loss of 5mC in KO1 occurred mainly in the repetitive fraction (40% loss of 5mC) (Fig. 1). The repetitive fraction contained genomic repeats such as satellite 2 (Sat2) and the ribosomal DNA repeat unit, whereas CpG islands of gene promoters were essentially contained in the CpG-rich fraction (see "Experimental Procedures"). Indeed, bisulfite genomic sequencing of the CpG-rich region at the 5′-end of the

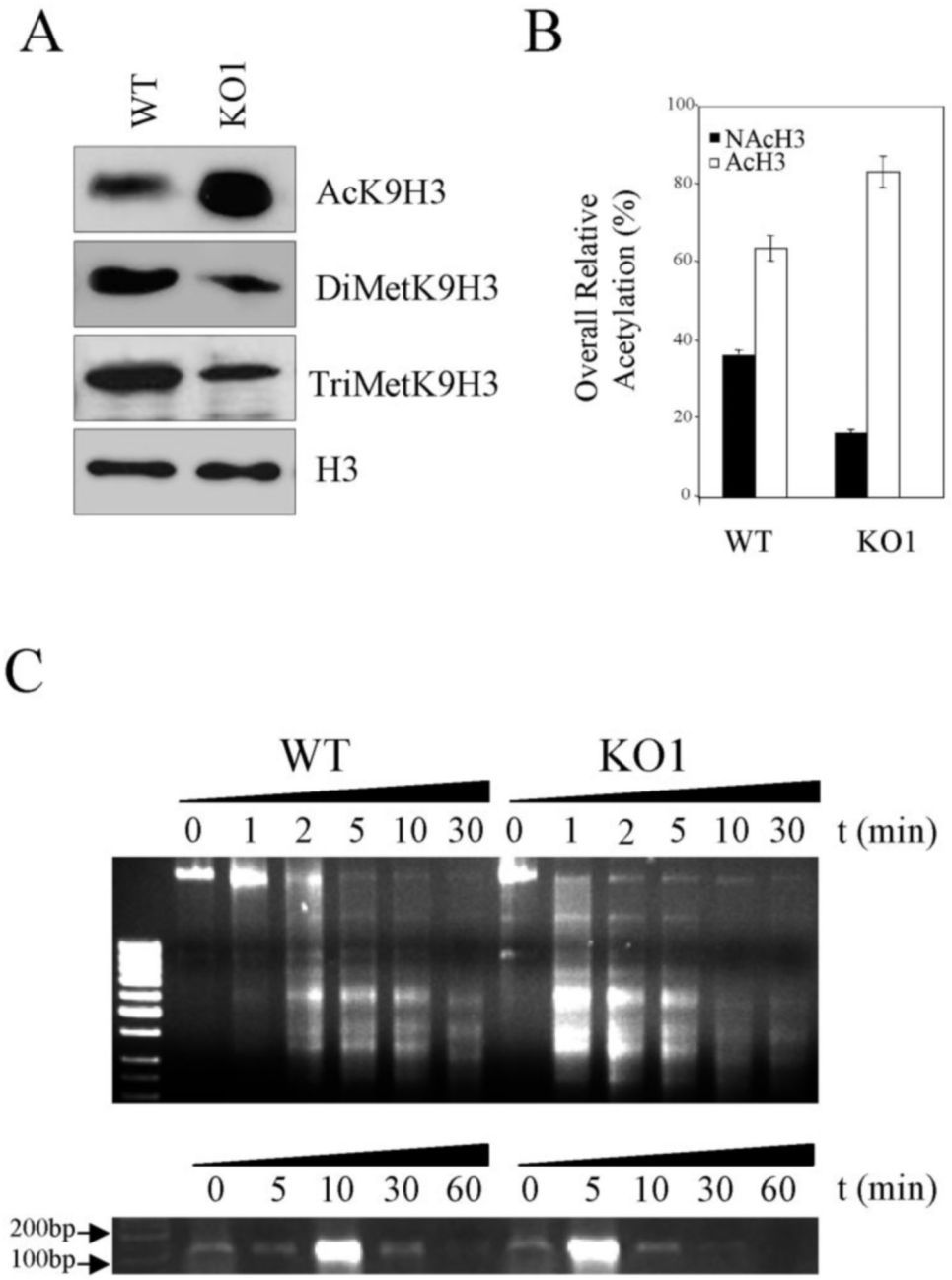

FIG. 4. **Hyperacetylation and accompanying loss of methylation of lysine 9 of histone H3 in human cells lacking DNMT1.** *A*, immunoblot analysis of nuclear proteins shows increased histone H3 lysine 9 acetylation (*AcK9H3*) and decreased levels of dimethyl lysine 9 H3 (*DiMetK9H3*) and trimethyl lysine 9 H3 (*TriMetK9H3*) in KO1 cells compared with WT cells. Histone H3 stained with an antibody raised against the unmodified C-terminal region of the protein is included as a loading control. *B*, HPCE quantitation of total nonacetylated (*NAc*) and acetylated (*Ac*) histone H3 revealed hyperacetylation in KO1 compared with WT cells. All results are representative of at least three replicates. *C*, analysis of chromatin accessibility using MNase digestions. KO1 cells showed a faster generation of discrete polynucleosomal subunits (*upper panel*), as well as an early release of mononucleosomal particles (*lower panel*).

28 S component of ribosomal DNA demonstrated that HCT-116 wild type cells are methylated at this region, whereas KO1 cells are hypomethylated (Fig. 1*B*). In fact, the D4Z4 locus, a polymorphic tandem repeat found to be hypomethylated in ICF (immunodeficiency, centromeric region instability and facial anomalies) syndrome patients harboring mutations in DNMT3b (26), mainly occurred within the CpG fraction. These results suggest a central role of DNMT1 in the methylation of specifically repetitive sequences, a role that is also supported by studies on mouse embryonic stem cells deficient in DNMT1 (27, 28).

Morphological Alterations in the Nucleus of Human Cells Lacking DNMT1—We next investigated the cytochemical distribution of 5mC in WT and KO1 cells. WT cells showed a punctated homogeneous distribution of 5mC throughout the nucleus (Fig. 2*A*). These cells also displayed a characteristic DAPI staining pattern consisting of discrete spots of strongly positive regions corresponding to the spatial arrangement of heterochromatin in the nucleus (Fig. 2*A*). Colocalization analysis in 0.2-μm thick confocal sections showed that the heterochromatic, DAPI-positive regions in WT cells were not associated with a particular pattern of 5mC distribution (Fig. 2*B*). On the contrary, KO1 cells showed a large intranuclear invagination after 5mC staining, often displaying a "doughnut"-like appearance with a central cavity lacking a positive signal and a punctated heterogeneous 5mC distribution in the rest of the

nucleus (Fig. 2*A*). This invagination, which is present in 80–90% of KO1 cells, traverses the nucleus (Fig. 2*C*) and is associated with a DAPI-negative region (Fig. 2, *A–C*). The pattern of DAPI staining also revealed an altered distribution of strongly DAPI-positive regions that became smaller and more diffuse in KO1 cells (Fig. 2*A*). Confocal analysis of 5mC and DAPI staining clearly revealed the diffuse and disorganized nature of heterochromatic DAPI-positive regions in KO1 cells. Again, in this case, these were not associated with a particular pattern of 5mC distribution (Fig. 2*B*).

To investigate a possible relationship between the appearance of an aberrant nuclear morphology in KO1 cells and alterations in the cell cycle, we performed a flow cytometry analysis of WT and KO1 cells. No significant differences were observed in the G_0/G_1 and S phase populations of WT and KO1 cells (Fig. 2*D*). We observed by FACS a small increase (6%) of the apoptotic (sub-G_0) population in KO1 cells compared with WT cells, corresponding to a very small population of cells according to the TUNEL assay. This extremely minor increase in the apoptotic population is highly unlikely to be responsible for the severe nuclear alteration observed in the KO1 cells.

To investigate further the morphological phenotype associated with the loss of DNMT1 in human cells, we performed an ultrastructural analysis of WT and KO1 cells. At the electron microscopic level, WT cells showed an entire nuclear envelope with no clear deformations in most cases (Fig. 3*A*). In these cells, one to three compact and spherical nucleolar masses, composed of a prominent granular region in which small fibrillar regions are embedded, were usually found in the nucleoplasm (Fig. 3*A*). By contrast, severe deformations and many deep and irregular folds on the nuclear envelope were found in most KO1 cells (Fig. 3, *A* and *B*). The nucleolar substructure was similar in KO1 and WT cells. However, in KO1 cells the nucleolar masses appeared distorted and segregated and were commonly attached to the invaginations of the nuclear envelope (Fig. 3, *A* and *B*). Therefore, the central cavity observed in 5mC and DAPI-stained KO1 nuclei corresponds to a great alteration in the nuclear architecture. The explanation that the appearance of the aberrant nuclear morphology in KO1 cells was an indirect effect of the loss of DNMT1 cannot be discounted at present. However, all the above results suggest an important role for DNMT1 in the maintenance of the structural nuclear arrangement.

Loss of DNMT1 in Human Cells Is Associated with Changes in the Histone H3 Modification Pattern—Given the tight connection between DNA methylation, histone modifications, and chromatin structure (12, 13, 29–31), it is plausible to expect changes in histone modifications in human cells with depleted DNMT1. In fact, complete removal of CpG methylation in plant cells results in a loss of histone H3 (H3) methylation at lysine 9 (11). Loss of acetylation and increased methylation at the Lys-9 residue of H3 have been associated with chromatin compaction and the formation of heterochromatin (14, 32). In particular, trimethylation of H3 at Lys-9 (TriMetK9H3) is a marker for constitutive heterochromatin (32). By using specific antibodies for DiMetK9H3 and TriMetK9H3 in immunoblot analysis of total protein extracts, we observed a strong decrease of both methylated Lys-9 H3 species in KO1 cells when compared with WT cells (Fig. 4*A*). Conversely, we observed the presence of higher levels of acetylated H3 in KO1 cells. In particular, by using HPLC-purified H3, an increase of about 30% in the H3 acetylation content of KO1 compared with WT cells was established (Fig. 4*B*). These results suggest that the loss of DNMT1 in human cells is associated with the disorganization of heterochromatin.

To investigate this matter further, we performed a comparative chromatin accessibility experiment using MNase digestions of KO1 and HCT116 cells. When isolating whole genomic DNA after different incubation times with MNase, we found KO1 to be more accessible to MNase than was HCT116. In fact, after 1 min of digestion, over 80% of the DNA was already in discrete polynucleosomal subunits for KO1 cells, whereas less than 20% of the DNA was digested in wild type cells (Fig. 4*C*). Moreover, when isolating the soluble fraction of chromatin after MNase digestion, KO1 cells exhibited a faster burst of mononucleosomal release (around 5 min of digestion compared with 10 min for wild type cells) (Fig. 4*C*), supporting the notion that chromatin in KO1 cells is more accessible, probably as a consequence of profound changes in heterochromatin organization.

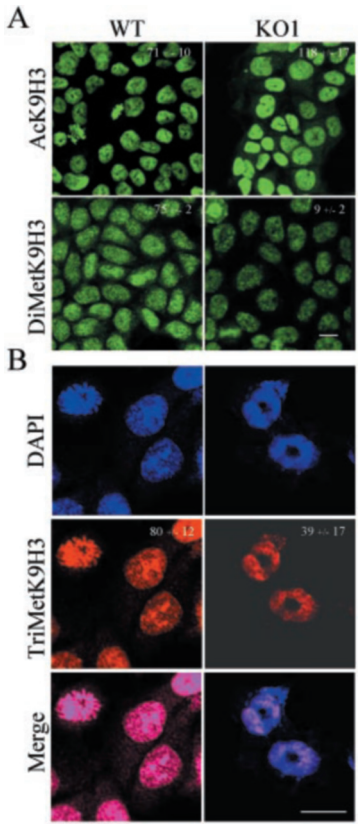

FIG. 5. **Quantitative and qualitative changes in the cellular distribution of methylated and acetylated forms of histone H3 in human cells lacking DNMT1.** *A*, analysis of AcK9H3 and DiMetK9H3 distribution in KO1 and WT cells by immunofluorescence microscopy. Numbers are the values of the integrated density of the total fluorescent emission per nuclear area of AcK9H3 and MetK9H3 signals in 50 nuclei from each replicate. Values are shown as averages (± S.D.) in arbitrary units of three replicates. *B*, confocal analysis of TriMetK9 (*red*) and DAPI-stained DNA (*blue*) shows altered distribution and disorganization in KO1 cells compared with WT cells. *Bars*, 10 μm.

At the cell level, immunolocalization analysis of the distribution of DiMetK9H3 and AcK9H3 in the nucleus of KO1 and WT cells suggested a quantitative switch rather than a qualitative change in spatial distribution of these two modified forms of H3 (Fig. 5). An optical measure of these observations by densitometric analysis showed a close agreement with the immunoblot and HPLC analysis described above (Figs. 4 and 5). These results confirmed at the cell level that lack of DNMT1 expression in human cancer cells is associated with a global nuclear change in the acetylation and methylation pattern of H3. The analysis of the distribution of TriMetK9H3 also indicated a quantitative diminution of this modified form of H3 in the nucleus of KO1 cells (Fig. 5). In addition, a change of the spatial localization of TriMetK9H3 was observed in KO1 cells.

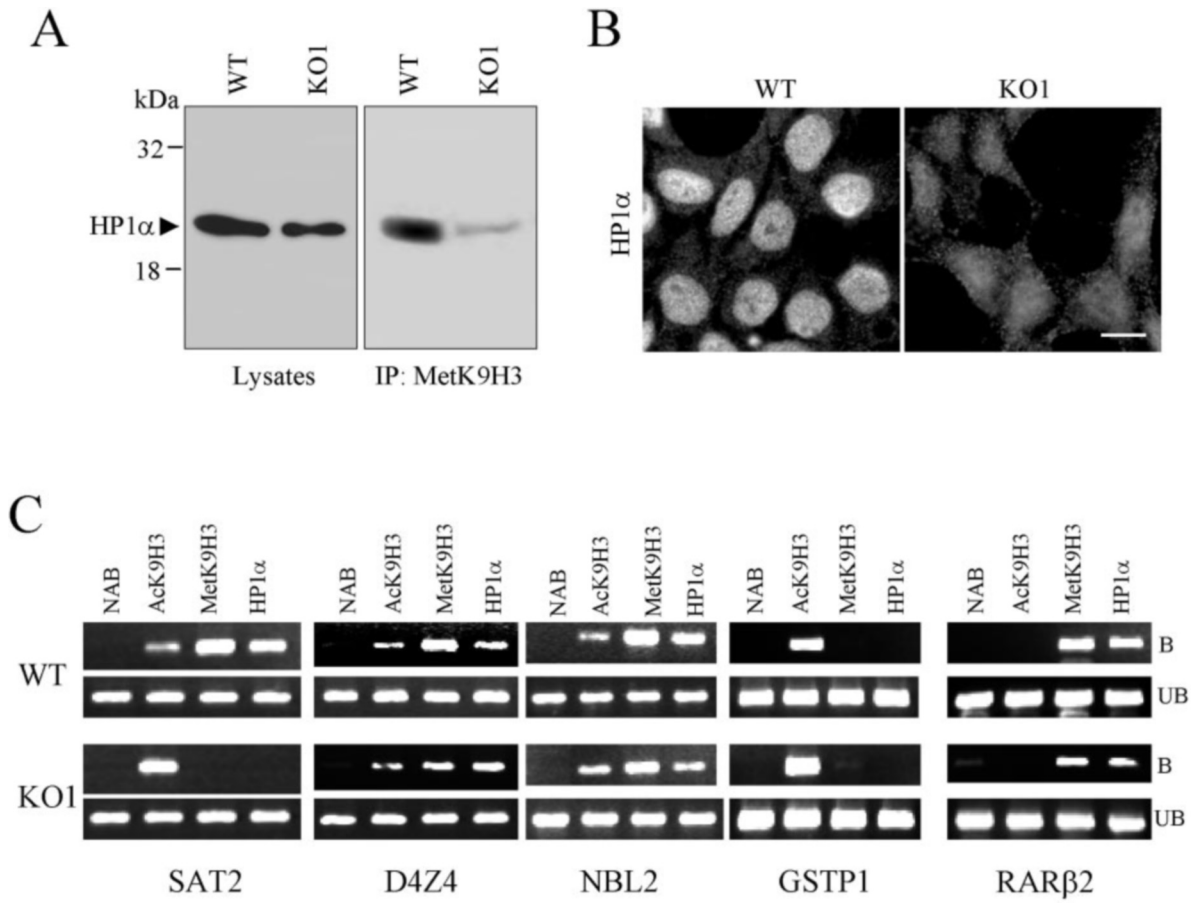

FIG. 6. **Loss of MetK9H3/HP1α interactions in human cells lacking DNMT1.** *A*, immunoprecipitation of HP1α with an anti-MetK9H3 antibody from KO1 and WT cells demonstrates loss of interaction in KO1 cells. Immunoprecipitates (*IP*) were analyzed by SDS-PAGE and immunoblotting with an antibody specific for HP1α. Total nuclear extracts (*lysates*) are included as input controls. Results shown are representative of three replicates. *B*, immunolocalization of HP1α in KO1 and WT cells reveals altered distribution in KO1 cells. *Bar*, 10 μm. *C*, ChIP assays showing interactions of Sat2, D4Z4, and NBL2 repeats and the promoter-CpG islands of inactive (*RARβ2*) and active (*GSTP1*) genes with AcK9H3, MetK9H3, and HP1α. Sat2 sequences interact with MetK9H3 and HP1α in WT but not in KO1 cells. Conversely, strong interaction of AcK9H3 with Sat2 repeats was observed in KO1 but not in WT cells. Similar patterns of association for D4Z4 and NBL2 repeats and the CpG islands of *RARβ2* and *GSTP1* were observed in WT and KO1 cells. A control reaction without antibody (*NAB*) was included. Panels show bound (*B*) and unbound (*UB*) fractions. Results are representative of at least two replicates.

Thus, the TriMetK9H3 signal was found mainly associated with discrete nuclear spots corresponding to DAPI-positive heterochromatin in WT cells (Fig. 5). However, a dispersed and diffused localization of TriMetK9H3 was observed in the nucleus of KO1 cells (Fig. 5), showing the disorganization of constitutive heterochromatin at the cell level.

Loss of the Interaction of HP1 with Methylated Lysine 9 at Histone H3 and with Repetitive Satellite 2 Genomic Sequences in Human Cells Lacking DNMT1—In human cells, methylation of histone H3 at Lys-9 by the site-specific histone methyltransferase (HMTase), Suv39h, creates a binding site for HP1 proteins (33, 34). Furthermore, interaction of HP1 and MetK9H3 is directly involved in heterochromatin formation and silencing of specific promoters (33, 34). We investigated the formation of the H3-HP1α complex in KO1 cells by protein immunoprecipitation of MetK9H3 (in all cases, similar results were obtained with both DiMetK9H3 and TriMetK9H3 antibodies). We found that the MetK9H3-HP1α protein complex was almost completely abrogated in KO1 cells (Fig. 6*A*). A quantitative decrease and a spatial disorganization of HP1α were also observed in many KO1 cells when compared with WT (Fig. 6, *A* and *B*). In order to further characterize the heterochromatin state in these cells, we performed ChIP assays with antibodies raised against DiMetK9H3 and TriMetK9H3 and AcK9H3 and HP1α proteins. Five types of genomic sequences were used in the immunoprecipitation analysis: Sat2 and nonsatellite D4Z4 and NBL2 repeats (26, 35) and the promoter-associated CpG islands of the active and inactive genes *GSTP1* and *RARβ2* (25). Sat2 sequences in pericentromeric heterochromatin have found to be hypomethylated by Southern blot in human cells lacking DNMT1 (4, 26), results that we have corroborated by using bisulfite genomic sequencing (data not shown). Methylation of D4Z4 and NBL2 repeats seems to be dependent on DNMT3b but not on DNMT1 activity (4, 26). Our analysis showed that the interaction of Sat2 sequences with both MetK9H3 (di- and trimethylation) and HP1α was impaired in the KO1 cells (Fig. 6*C*). Conversely, AcK9H3 was associated with Sat2 repeats in KO1 cells but highly reduced in WT cells (Fig. 6*C*). In contrast, we observed similar patterns of association for AcK9H3, MetK9H3, and HP1α with D4Z4 and NBL2 repeats and the promoter-CpG island of inactive (*RARβ2*) and active (*GSTP1*) genes in WT and KO1 cells (Fig. 6*C*). Collectively, these results indicate that the absence of DNMT1 in human cells can alter the organization of specific genomic regions.

Loss of the Interaction of HDAC1 and HDAC2 with Repetitive Satellite 2 Genomic Sequences in Human Cells Lacking DNMT1—DNMTs (13, 31) and methyl-CpG-binding proteins (36, 37) have been shown to recruit HDACs to methylated DNA. In particular, interactions of DNMT1 with both HDAC1 and HDAC2 have been described recently (13, 31, 38). Recruitment of HDACs to methylated DNA has been associated with

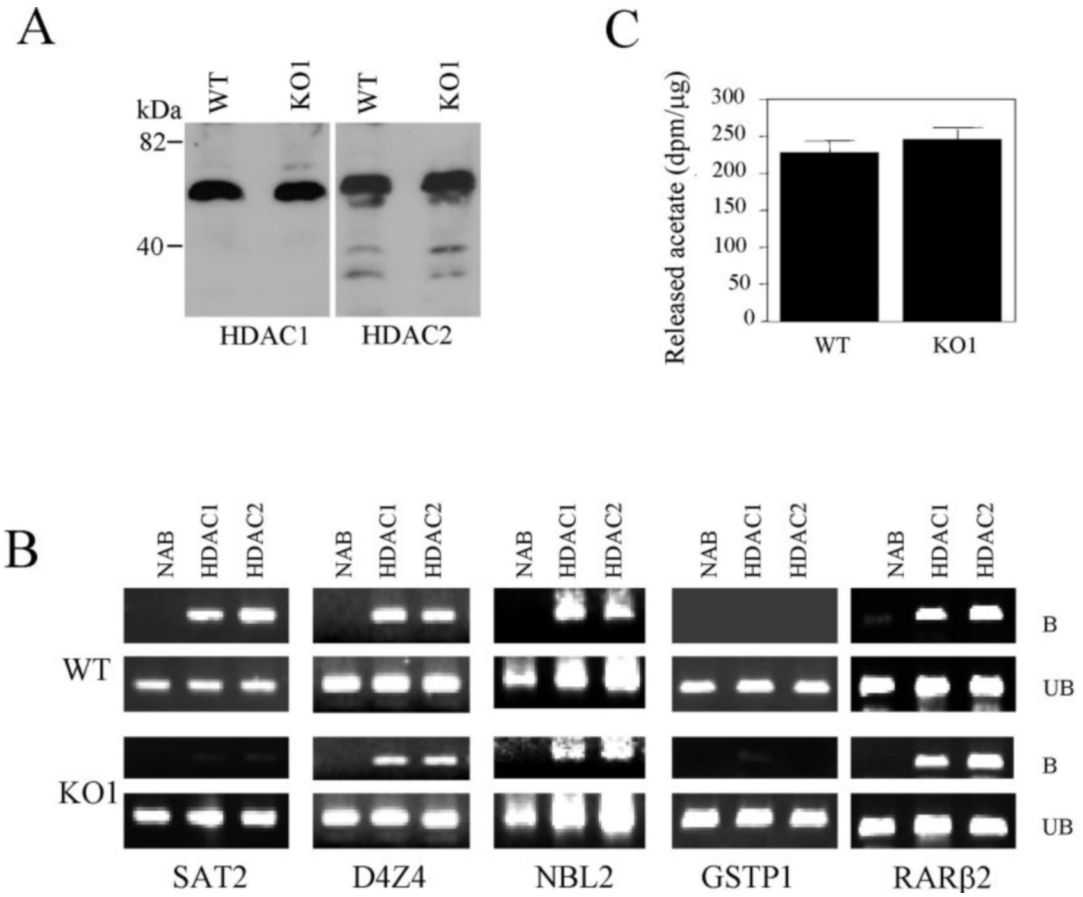

FIG. 7. **ChIP of HDACs and HDAC activity.** *A*, immunoblot analysis of nuclear protein extracts showing the expression pattern of HDAC1 and -2 in WT and KO1 cells. *B*, ChIP assay showing interactions of HDAC1 and HDAC2 with Sat2, D4Z4, and NBL2 repeats and the silenced *RARβ2* promoter-CpG island in WT and KO1 cells. HDAC1 and HDAC2 associate with D4Z4 and NBL2 repeats and the CpG island of the inactive gene *RARβ2* in WT and KO1 cells in contrast to Sat2 repeats, where the interaction of both HDACs was greatly reduced in KO1 cells. HDCAs are not present in the CpG island of the active gene *GSTP1* of WT and KO1 cells. The panels are labeled as above. Results are representative of at least two replicates. *C*, measurement of total HDAC activity reveals similar overall values for both WT and KO1 cells. HDAC activity was determined by measuring released [^{3}H]acetate in a scintillation counter after incubation of nuclear extracts with ^{3}H-labeled histones (7).

transcriptional repression and the formation of heterochromatic DNA. Thus, we investigated the possible interactions of HDACs 1 and 2 with specific DNA sequences. We found a specific interaction between HDAC1 and HDAC2 with Sat2, D4Z4, and NBL2 repeats and the promoter-CpG island of the inactive gene *RARβ2* in WT cells (Fig. 7*B*). HDAC1 and HDAC2 did not interact with the CpG island of the active gene *GSTP1* (Fig. 7*B*). In agreement with the switch in the K9H3 modification pattern observed, the interaction of HDAC1 and HDAC2 with Sat2 repeats (but not with D4Z4 and NBL2 repeats or the inactive *RARβ2* gene) is impaired in KO1 cells (Fig. 7). The absence of DNMT1 and subsequent hypomethylation of Sat2 repeats could result in the loss of direct recruitment of HDACs to target DNA sequences by either DNMT1 (13, 31) or methyl-CpG-binding proteins (36, 37). Thus, the hyperacetylation of H3 in KO1 cells may be the result of a loss of targeted HDAC activity at specific DNA sequences rather than a loss of overall HDAC activity. This notion is supported by our analysis of overall HDAC enzyme activity, which did not reveal any differences between WT and KO1 cells (Fig. 7*C*).

Expression of Murine DNMT1 in Human Cells Lacking DNMT1 Restores a WT-like Phenotype—To demonstrate further the involvement of DNMT1 in the maintenance of the H3 modification pattern, we transfected a cDNA encoding the murine DNMT1 in KO1 cells. This resulted in a significant expression of DNMT1 (Fig. 8*A*) that was associated with the reestablishment of the pattern of acetylated and methylated forms of H3 observed in WT cells (Fig. 8*A*). Analyzing the cell morphology of the transfected pool revealed a significant increase, 60% in relation to those cells transfected with the empty vector, in the number of cells with a nuclear architecture resembling the WT phenotype. In detail, KO1 cells transfected with DNMT1 displayed a characteristic DAPI-staining pattern consisting of discrete spots of strongly positive regions with a normal nuclear morphology lacking the central cavity characteristic of KO1 cells (Fig. 8*B*). Furthermore, the DNMT1-transfected KO1 cells display a localization of TriMetK9H3 and HP1α in discrete nuclear spots corresponding to DAPI-positive heterochromatin, in contrast to the diffuse distribution of TriMetK9H3 and HP1α in the KO1 cells (Fig. 8*B*). HCT-116 cells transfected with the empty vector did not show any evidence of these changes.

DISCUSSION

The results presented here suggest, at least in our model, the existence of two phenotypes associated with the loss of DNMT1 in human cells: aberrant alterations of nuclear architecture and an overall change in the histone H3 modification pattern. Similar gross changes in nuclear morphology have not been observed in mouse embryonic stem cells lacking DNMT1 (12). However, changes in nuclear morphology and in 5mC distribution resembling those of KO1 cells have been found in other human cancer cells and in a mouse tumor progression model (39, 40). This raises the possibility that the nuclear morphology observed in KO1 cells is an indirect effect of the loss of DNMT1 in the context of cancer. In any case, as the changes in nuclear

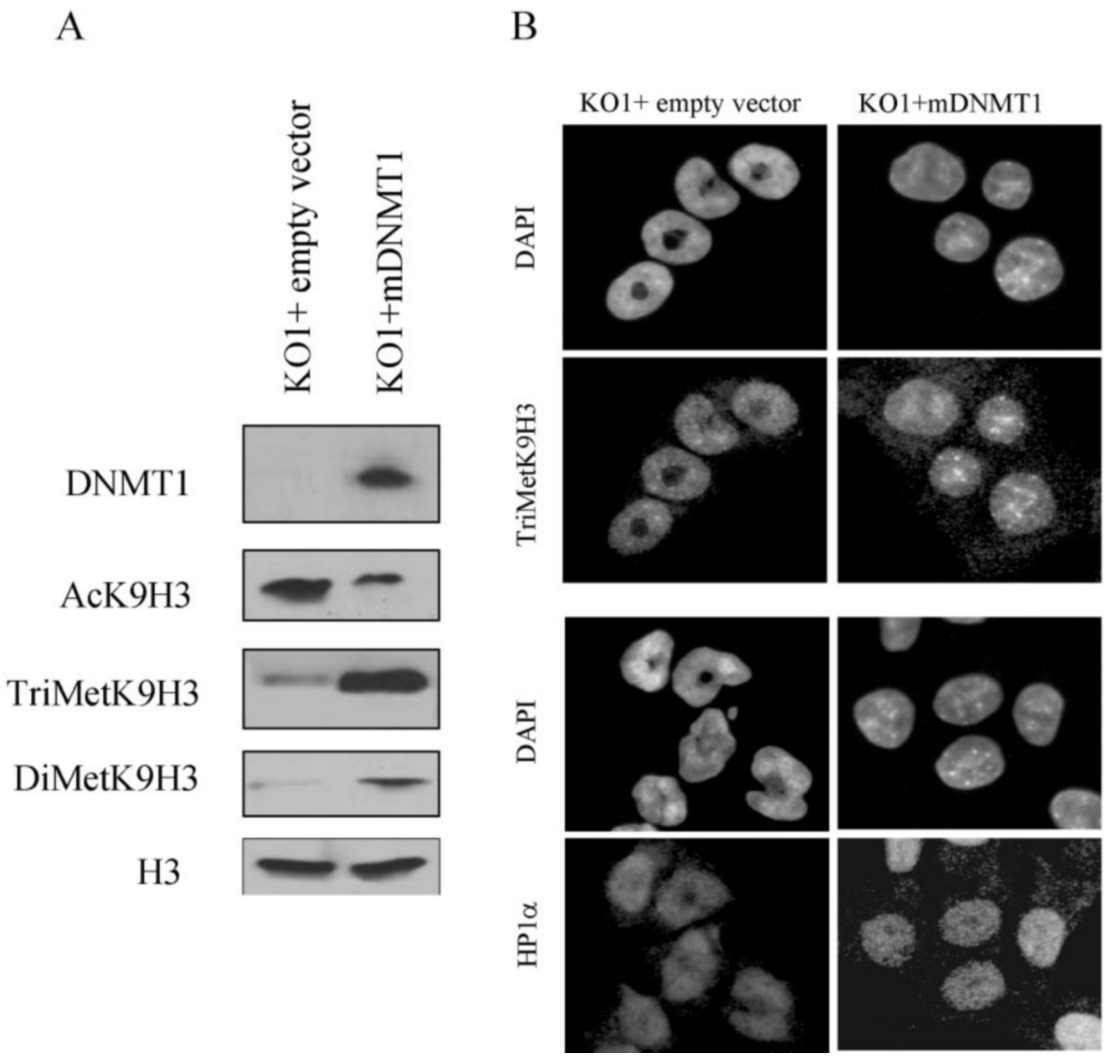

FIG. 8. **Expression of murine DNMT1 in KO1 cells restores a WT-like phenotype.** *A*, Western blots in KO1 cells and KO1 cells transfected with the DNMT1 vector. Cells were harvested 48 h post-transfection. Whole-cell lysates were prepared, analyzed by SDS-PAGE, and immunoblotted with the indicated antibodies. Histone H3 stained with an antibody raised against the unmodified C-terminal region of the protein are included as a loading control. *B*, DAPI staining and immunofluorescence localization of TriMetK9H3 (*upper panels*) and HP1α (*lower panels*) in KO1 cells (*left column*) and KO1 cells transfected with murine DNMT1 (*right column*) showing the restoration of a WT-like phenotype.

morphology exclusively depend on the loss of DNMT1, these observations suggest that DNMT1 is an important element in the organization of chromatin domains inside the cell nucleus.

At this point it is difficult to have a clear idea of the mechanism underlying the effects on nuclear organization that may be attributed to the removal of DNMT1. Nevertheless, given the gross nuclear alteration of KO1 cells, it is tempting to speculate that large and definite nuclear domains or structures are the underlying targets involved. In interphase chromosomes, large regions, such as centromeres and telomeres, occupy discrete nonoverlapping territories, and evidence suggests that their position within the nucleus is organized nonrandomly, and hence they might be of functional significance (5). In particular, centromeric regions tend to associate giving rise to a definite nuclear domain known as the chromocenter (6). There is also evidence to suggest that the major sequence targets of DNMT1 are located in large pericentromeric regions (4). Moreover, inside the nucleolus, the most prominent intranuclear structure, human repetitive ribosomal RNA genes are targets for DNA methylation (41), and our preliminary findings indicate that these regions undergo demethylation in KO1 cells.

The second set of changes observed in KO1 cells corresponds to a global change in the histone H3 modification pattern. Increasing evidence linking human DNMT1 with both HDAC and SUV39H1 HMTases may explain these changes in the H3 modification pattern both at a genomic level and at that of particular genetic sequences. The associations between DNMT1 and HDAC activity are well established (13, 31, 38), and our results show the physiological consequences of the abrogation of this connection at both a global level and within a specific sequence context. Furthermore, recent evidence from MEFs indicates that Suv39h-mediated K9H3 methylation may direct DNA methylation to major satellite repeats in pericentric heterochromatin (12). Most interestingly, in this MEF context, these effects of Suv39h depend on trimethylation of K9H3 and may require DNMT3b rather than DNMT1 (12). However, as we have observed that DNMT1 is necessary to maintain trimethylation of Lys-9 at histone H3 at pericentromeric regions in human cancer cells, it may be that a different HMTase or abnormal HMTase targeting is characteristic of the cancer transformation (42, 43). Related to this issue, it was already known that the double genetic disruption of DNMT1 and DNMT3b in these cancer cells induced acetylation of histone H4 and loss of DiMetK9H3 (44, 45). Alternatively, the MEF results may be explained by the well known interspecific differences in chromatin structure, CpG island distribution, and HP1α localization between human and mouse (46, 47). Con-

cerning this latter issue, whereas mouse DNMT1 loss results in ectopic gene expression that is associated with demethylation at unique sequences (48, 49), we and other researchers have not found demethylation at unique CpG islands in these human cancer cells that are genetically defective in DNMT1 (4, 25, 44) or DNMT1 depleted by RNAi (50). The only exception is the report by Robert *et al.* (51), who claimed to have identified gene-specific demethylation using antisense and RNAi methodology to deplete DNMT1. Most importantly, the loss of methylation from repetitive sequences in the KO1 cells, such as the satellite 2 tandem repeat or the 28 S ribosomal DNA loci, seems to be the most important DNA hypomethylation event in our study. This can clearly be related to the changes in the structure of chromatin and the nucleus.

Although it is not possible to conclude with certainty that the two major phenotypes we have described in KO1 cells are directly connected, there is growing evidence to indicate that nuclear organization and chromatin modifications are directly related (6). It is therefore a reasonable hypothesis that global changes in histone H3 modification status, as a consequence of DNMT1 loss, have some connection with the alteration of nuclear organization. A recent report provides an example of a single nuclear protein (SATB1) establishing a tight connection between gene regulation, nuclear architecture, and histone H3 modifications (52). The data presented here support this hypothesis and suggest that the maintenance of distinct/discrete regions of genomic DNA methylation by DNMT1 contributes to the adoption of the appropriate chromatin organization within the cell.

Acknowledgments—We thank Dr. Bert Vogelstein for kindly providing the wild type and KO1 HCT-116 cell lines used in the study, Dr. Thomas Jenuwein for providing the trimethyl-Lys-9 histone H3 antibody, and Dr. Kevin Petrie for editorial assistance.

REFERENCES

1. Bestor, T. H. (2000) *Hum. Mol. Genet.* **9,** 2395–2402
2. Li, E., Bestor, T. H., and Jaenisch, R. (1992) *Cell* **69,** 915–926
3. Okano, M., Bell, D. W., Haber, D. A., and Li, E. (1999) *Cell* **99,** 247–257
4. Rhee, I., Jair, K. W., Yen, R. W., Lengauer, C., Herman, J. G., Kinzler, K. W., Vogelstein, B., Baylin, S. B., and Schuebel, K. E. (2000) *Nature* **404,** 1003–1007
5. Cremer, T., and Cremer, C. (2001) *Nat. Rev. Genet.* **2,** 292–301
6. Francastel, C., Schubeler, D., Martin, D. I., and Groudine, M. (2000) *Nat. Rev. Mol. Cell. Biol.* **1,** 137–143
7. Jenuwein, T., and Allis, C. D. (2001) *Science* **293,** 1074–1080
8. Strahl, B. D., and Allis, C. D. (2000) *Nature* **403,** 41–45
9. Trouche, D., Khochbin, S., and Dimitrov, S. (2003) *Cell* **12,** 281–286
10. Turner, B. M. (2000) *BioEssays* **22,** 836–845
11. Tariq, M., Saze, H., Probst, A. V., Lichota, J., Habu, Y., and Paszkowski, J. (2003) *Proc. Natl. Acad. Sci. U. S. A.* **100,** 8823–8827
12. Lehnertz, B., Ueda, Y., Derijck, A. A. H. A., Braunschweig, U., Perez-Burgos, L., Kubicek, S., Chen, T., Li, E., Jenuwein, T., and Peters A. H. (2003) *Curr. Biol.* **13,** 1192–1200
13. Fuks, F., Burgers, W. A., Brehm, A., Hughes-Davies, L., and Kouzarides, T. (2000) *Nat. Genet.* **24,** 88–91
14. Peters, A. H., Kubicek, S., Mechtler, K., O'Sullivan, R. J., Derijck, A. A., Perez-Burgos, L., Kohlmaier, A., Opravil, S., Tachibana, I., Shinkai, Y., Martens, J. H., and Jenuwein, T. (2003) *Mol. Cell* **12,** 1577–1589
15. Espada, J., Perez-Moreno, M., Braga, V. M., Rodriguez-Viciana, P., and Cano, A. (1999) *J. Cell Biol.* **146,** 967–980
16. Ballestar, E., Paz, M. F., Valle, L., Wei, S., Fraga, M. F., Espada, J, Cigudosa, J. C., Huang, T. H.-M., and Esteller, M. (2003) *EMBO J.* **22,** 6335–6345
17. Fournier, C., Goto, Y., Ballestar, E., Delaval, K., Hever, A. M., Esteller, M., and Feil, R. (2002) *EMBO J.* **21,** 6560–6570
18. Kurdistani, S. K., Robyr, D., Tavazoie, S., and Grunstein, M. (2002) *Nat. Genet.* **31,** 248–254
19. Habib, M., Fares, F., Bourgeois, C. A., Bella, C., Bernardino, J., Hernandez-Blazquez, F., de Capoa, A., and Niveleau, A. (1999) *Exp. Cell Res.* **249,** 46–53
20. Lindner, H., Helliger, W., Dirschlmayer, A., Jaquemar, M., and Puschendorf, B. (1992) *Biochem. J.* **283,** 467–471
21. Weintraub, H., Palter, K., and Van Lente, F. (1975) *Cell* **6,** 83–88
22. Fraga, M. F., Uriol, E., Borja, D. L., Berdasco, M., Esteller, M., Canal, M. J., and Rodriguez, R. (2002) *Electrophoresis* **23,** 1677–1681
23. Cross, S. H., Charlton, J. A., Nan, X., and Bird, A. P. (1994) *Nat. Genet.* **6,** 236–244
24. Huang, T. H., Perry, M. R., and Laux, D. E. (1999) *Hum. Mol. Genet.* **8,** 459–470
25. Paz, M. F., Wei, S., Cigudosa, J. C., Rodriguez-Perales, S., Peinado, M. A., Huang, T. H., and Esteller, M. (2003) *Hum. Mol. Genet.* **12,** 2209–2219
26. Kondo, T., Kondo, T., Bobek, M. P., Kuick, R., Lamb, B., Zhu, X., Narayan, A., Bourc'his, D., Viegas-Pequignot, E., Ehrlich, M., and Hanash, S. M. (2000) *Hum. Mol. Genet.* **9,** 597–604
27. Liang, G., Chan, M. F., Tomigahara, Y., Tsai, Y. C., Gonzales, F. A., Li, E., Laird, P. W., and Jones, P. A. (2002) *Mol. Cell. Biol.* **22,** 480–491
28. Woodcock, D. M., Linsenmeyer, M. E., and Warren, W. D. (1998) *Gene* (*Amst.*) **206,** 63–67
29. Ballestar, E., and Esteller, M. (2003) in *Nature Encyclopedia of the Human Genome* (Cooper, D. N., ed) Vol. 2, pp. 114–118, Nature Publishing Group, London
30. Fuks, F., Hurd, P. J., Deplus, R., and Kouzarides, T. (2003) *Nucleic Acids Res.* **31,** 2305–2312
31. Rountree, M. R., Bachman, K. E., and Baylin, S. B. (2000) *Nat. Genet.* **25,** 269–277
32. Peters, A. H., Mermoud, J. E., O'Carroll, D., Pagani, M., Schweizer, D., Brockdorff, N., and Jenuwein, T. (2002) *Nat. Genet.* **30,** 77–80
33. Bannister, A. J., Zegerman, P., Partridge, J., Miska, E. A., Thomas, J. O., Allshire, R. C., and Kouzarides, T. (2001) *Nature* **410,** 120–124
34. Lachner, M., O'Carroll, D., Rea, S., Mechtler, K., and Jenuwein, T. (2001) *Nature* **410,** 116–120
35. Lyle, R., Wright, T. J., Clark, L. N., and Hewitt, J. E. (1995) *Genomics* **28,** 389–397
36. Jones, P. L., Veenstra, G. J., Wade, P. A., Vermaak, D., Kass, S. U., Landsberger, N., Strouboulis, J., and Wolffe, A. P. (1998) *Nat. Genet.* **19,** 187–191
37. Nan, X., Ng, H. H., Johnson, C. A., Laherty, C. D., Turner, B. M., Eisenman, R. N., and Bird, A. (1998) *Nature* **393,** 386–389
38. Robertson, K. D., Ait-Si-Ali, S., Yokochi, T., Wade, P. A., Jones, P. L., and Wolffe, A. P. (2000) *Nat. Genet.* **25,** 338–342
39. Hernández-Blazquez, F. J., Habib, M., Dumollard, J. M., Barthelemy, C., Benchaib, M., de Capoa, A., and Nivelau, A. (2000) *Gut* **47,** 689–693
40. Veilleux, C., Bernardino, J., Gibaud, A., Nivelau, A., Malfoy, B., Dutrillaux, B., and Burgois, C. A. (1995) *Bull. Cancer* (*Paris*) **82,** 939–945
41. Brock, G. C., and Bird, A. (1997) *Hum. Mol. Genet.* **6,** 451–456
42. Huang, S. (2002) *Nat. Rev. Cancer* **2,** 469–476
43. Schneider, R., Bannister, A. J., and Kouzarides, T. (2002) *Trends Biochem. Sci.* **27,** 396–402
44. Rhee, I., Bachman, K. E., Park, B. H., Jair, K. W., Yen, R. W., Schuebel, K. E., Cui, H., Feinberg, A. P., Lengauer, C., Kinzler, K. W., Baylin, S. B., and Vogelstein, B. (2002) *Nature* **416,** 552–556
45. Bachman, K. E., Park, B. H., Rhee, I., Rajagopalan, H., Herman, J. G., Baylin, S. B., Kinzler, K. W., and Vogelstein, B. (2003) *Cancer Cell* **3,** 89–95
46. Cross, S. H., Lee, M., Clark, V. H., Craig, J. M., Bird, A. P., and Bickmore, W. A. (1997) *Genomics* **40,** 454–461
47. Minc, E., Allory, Y., Workman, H. J., Courvalin, J. C., and Buendia, B. (1999) *Chromosoma* (*Berl.*) **108,** 220–234
48. Jackson-Grusby, L., Beard, C., Possemato, R., Tudor, M., Fambrough, D., Csankovszki, G., Dausman, J., Lee, P., Wilson, C., Lander, E., and Jaenisch, R. (2001) *Nat. Genet.* **27,** 31–39
49. Warnecke, P. M., Biniszkiewicz, D., Jaenisch, R., Frommer, M., and Clark, S. J. (1998) *Dev. Genet.* **22,** 111–121
50. Ting, A. H., Jair, K., Suzuki, H., Yen, R. W., Baylin, S. B., and Schuebel, K. E. (2004) *Nat. Genet.* **36,** 582–584
51. Robert, M. F., Morin, S., Beaulieu, N., Gauthier, F., Chute, I. C., Barsalou, A., and MacLeod, A. R. (2003) *Nat. Genet.* **33,** 31–35
52. Cai, S., Han, H.-J., and Kohwi-Shigematsu, T. (2003) *Nat. Genet.* **34,** 42–51